

# SCIENTIFIC REPORTS



OPEN

## Characterisation of *Plasmodium falciparum* populations selected on the human endothelial receptors P-selectin, E-selectin, CD9 and CD151

Nahla Galal Metwally<sup>1,2</sup>, Ann-Kathrin Tilly<sup>1</sup>, Pedro Lubiana<sup>1</sup>, Lisa K. Roth<sup>1</sup>, Michael Dörpinghaus<sup>1</sup>, Stephan Lorenzen<sup>1</sup>, Kathrin Schuldt<sup>1</sup>, Susanne Witt<sup>1</sup>, Anna Bachmann<sup>1</sup>, Henning Tidow<sup>3</sup>, Thomas Gutschmann<sup>4</sup>, Thorsten Burmester<sup>5</sup>, Thomas Roeder<sup>6</sup>, Egbert Tannich<sup>1</sup> & Iris Bruchhaus<sup>1</sup>

The ability of the parasite *Plasmodium falciparum* to evade the immune system and be sequestered within human small blood vessels is responsible for severe forms of malaria. The sequestration depends on the interaction between human endothelial receptors and *P. falciparum* erythrocyte membrane protein 1 (PfEMP1) exposed on the surface of the infected erythrocytes (IEs). In this study, the transcriptomes of parasite populations enriched for parasites that bind to human P-selectin, E-selectin, CD9 and CD151 receptors were analysed. IT4\_var02 and IT4\_var07 were specifically expressed in IT4 parasite populations enriched for P-selectin-binding parasites; eight *var* genes (IT4\_var02/07/09/13/17/41/44/64) were specifically expressed in isolate populations enriched for CD9-binding parasites. Interestingly, IT4 parasite populations enriched for E-selectin- and CD151-binding parasites showed identical expression profiles to those of a parasite population exposed to wild-type CHO-745 cells. The same phenomenon was observed for the 3D7 isolate population enriched for binding to P-selectin, E-selectin, CD9 and CD151. This implies that the corresponding ligands for these receptors have either weak binding capacity or do not exist on the IE surface. Conclusively, this work expanded our understanding of *P. falciparum* adhesive interactions, through the identification of *var* transcripts that are enriched within the selected parasite populations.

*Plasmodium falciparum* is responsible for most of the morbidity and mortality accompanying malaria in humans. According to the World Health Organisation, 212 million cases were reported globally in 2015 with an estimated 429,000 deaths<sup>1</sup>.

The ability of *P. falciparum*-infected erythrocytes (IEs) to evade the immune system and be sequestered in small blood vessels of vital organs constitutes the major virulence attribute<sup>2,3</sup>. IE sequestration underpins the most severe pathological phenotypes observed in malaria, including blood flow obstruction, hypoxia, induction of inflammatory immune responses, endothelial dysfunction, tissue damage and, ultimately, organ failure<sup>2,4-6</sup>.

The success of *P. falciparum* as a parasite of humans is attributed to the presence of variant surface antigens (VSAs) on the IE surface. These antigens are encoded by five large multi-copy gene families, namely, the *var*, *rif* (repetitive interspersed family), *stevor* (subtelomeric variable open read frame), *surf* (surface-associated

<sup>1</sup>Bernhard Nocht Institute for Tropical Medicine, Hamburg, Germany. <sup>2</sup>Medical Parasitology Department, Faculty of Medicine-Suez Canal University, Ismailia, Egypt. <sup>3</sup>Department of Chemistry, Institute for Biochemistry and Molecular Biology, University of Hamburg, Hamburg, Germany. <sup>4</sup>Division of Biophysics, Research Center Borstel, Leibniz-Center for Medicine and Biosciences, Borstel, Germany. <sup>5</sup>Institute of Zoology, Biocenter Grindel, University of Hamburg, Hamburg, Germany. <sup>6</sup>Zoological Institute, Department of Molecular Physiology, Christian-Albrechts University Kiel, Kiel, Germany. Nahla Galal Metwally and Ann-Kathrin Tilly contributed equally to this work. Correspondence and requests for materials should be addressed to I.B. (email: [bruchhaus@bnitm.de](mailto:bruchhaus@bnitm.de))

interspersed), and *Pfmc-2tm* (*P. falciparum* Maurer's cleft 2 transmembrane) multi-copy gene families. Their gene products are *P. falciparum* erythrocyte membrane protein 1 (*PfEMP1*), RIFIN, STEVOR, SURFIN and *PfMC-2TM* proteins, respectively<sup>7–12</sup>.

*PfEMP1* proteins play a major role in cytoadhesion and antigenic variation of IEs. The *PfEMP1*-encoding *var* genes vary greatly from parasite to parasite, giving rise to an enormous repertoire of *var* genes in nature<sup>8,13–16</sup>. The expression of *var* genes is mutually exclusive in ring-stage parasites, so that only one *PfEMP1* variant is localised on the IE surface at any given time<sup>17</sup>. *PfEMP1* proteins consist of a single intracellular domain, a transmembrane domain, and several extracellular Duffy binding-like (DBL) domains ( $\alpha$ ,  $\beta$ ,  $\gamma$ ,  $\delta$ ,  $\zeta$ , and  $\epsilon$ ) and cysteine-rich inter-domain regions (CIDR) ( $\alpha$ ,  $\beta$  and  $\gamma$ )<sup>18–20</sup>. *PfEMP1* proteins can be classified into groups A, B, B/A, C, B/C or E, depending on the chromosomal localisation of the encoding gene, the upstream sequences and *PfEMP1* domain composition<sup>8,21–23</sup>. In addition, an analysis of 399 different *PfEMP1* sequences from seven *P. falciparum* genomes allowed the identification of 23 domain cassettes (DCs)<sup>24</sup>.

At least 23 human endothelial receptors or structures interact with IEs<sup>3,25–30</sup>. Nevertheless, interactions with only a few human endothelial receptors, particularly CD36, intercellular adhesion molecule-1 (ICAM-1) and endothelial protein C receptor (EPCR), have been studied in detail.

Over 80% of *PfEMP1* proteins of the *P. falciparum* isolates 3D7 and IT4 contain CIDR $\alpha$ 2–6 domains, which are involved in CD36 binding<sup>31</sup>. EPCR was identified as the endothelial receptor of DC8-*PfEMP1* and DC13-*PfEMP1* (CIDR $\alpha$ 1 domain)<sup>26,32</sup>. In fact, the binding of CIDR $\alpha$ 1 to EPCR is associated with severe malaria<sup>26,33</sup>, and recent studies indicated that the main *Plasmodium var* transcript in severe paediatric malaria patients encodes protein domains predicted to bind EPCR<sup>34,35</sup>. ICAM-1 binding is linked to the DBL $\beta$ 3 within DC4-*PfEMP1* of group A proteins and to the DBL $\beta$ 5 domains of group B and C proteins<sup>20,36–39</sup>. In addition, DC5-*PfEMP1* was found to be responsible for the binding to PECAM-1<sup>29</sup>.

IEs also bind to P- and E-selectins<sup>40–44</sup> and *PfEMP1* was suggested to be the interacting partner<sup>45</sup>; however, other studies with various *P. falciparum* isolates did not reproduce E-selectin binding<sup>42,46</sup>. Recently, two tetraspanins, CD9 and CD151, were shown to interact with IEs<sup>25</sup>, but the identities of their binding partners are unknown.

The current study aimed to identify the as yet unknown ligands of *P. falciparum* that interact with the human receptors P-selectin, E-selectin, CD9 and CD151. Specifically expressed *var* genes were identified within parasite populations enriched for CD9 and P-selectin binding. However, the expression profiles of populations enriched for parasites binding to E-selectin and CD151 were identical to the expression profiles of parasite population exposed to wild-type CHO-745 cells.

## Results

**Endothelial receptor-binding capacity of *P. falciparum* isolates IT4 and 3D7.** To identify the putative *PfEMP1* ligands responsible for IE binding to various human receptors, the receptors were expressed on the surface of CHO-745 cells, and transcriptomes of ring-stage parasite populations enriched for parasites binding to these receptors were analysed.

In the first stage of analyses, the basic binding capacity of two laboratory strains, IT4 and 3D7, to the receptors of interest was evaluated. Static cytoadhesion assays were performed using trophozoite-stage IEs and transgenic CHO-745 cells with endothelial receptors expressed on their surface as green fluorescent protein (GFP) fusions (Fig. 1, Supplementary Fig. S1A–S1D and Fig. S2). Even after long-term cultivation, large number of *P. falciparum* IT4 parasites could bind to the endothelial cell receptor CD36 even without enrichment (Fig. 1A, Supplementary Fig. S1A) and, on average, 209 bound IEs per 100 CHO-745 cells were detected. Approximately 36 IEs were bound per 100 CHO745 cells expressing ICAM-1 (Fig. 1A and Supplementary Fig. S1B). By comparison, the binding capacity for the other studied receptors and for CHO-745 WT cells was very low. In the case of these receptors, no more than 5 IEs were bound per 100 receptor-expressing CHO-745 cells (Fig. 1A and Supplementary Fig. S1C, S1D). The CD36-binding capacity of *P. falciparum* 3D7 parasites after long-term culture without enrichment was lower than that of the IT4 isolate (Fig. 1B); on average, 140 bound IEs per 100 CHO-745 cells were observed. For all the other receptors studied, including ICAM-1, corresponding to no more than 6 IEs per 100 CHO-745 cells, was observed.

Because of the low proportion of IEs that were able to bind to ICAM-1, P-selectin, E-selectin, CD9 and CD151, parasite populations were then enriched for parasites with a higher capacity to bind to these receptors through repeated rounds of panning assays.

In parallel, we performed enrichment of parasite binding to CHO-745 WT cells. After the first round of selection, an interesting observation was the accumulation of IEs on large, morphologically abnormal CHO-745 cells. These so called “senescent” cells are always present in very low amounts in any normal culture<sup>47,48</sup>. In subsequent rounds of enrichment, the number of CHO-745-attached IEs increased dramatically (Supplementary Fig. S3A–S3D).

The binding capacity of the various enriched parasite populations was then investigated. As shown in Fig. 1A and B, high numbers of IEs infected by isolate IT4 or 3D7 bound CD36-expressing CHO-745 cells and a further increase of binding was not possible by continued enrichment. For all other analysed receptors and for CHO-745 WT cells, the number of bound IEs increased significantly (44–228 IT4-IEs/100 CHO-745 cells, and 15–140 3D7-IEs/100 CHO-745 cells).

***var* gene expression profiles in enriched IT4 parasite populations.** To identify *var* transcripts produced specifically in enriched parasite populations, three IE populations were generated. The first population comprised parasites after long-term culturing that were representative of the overall parasite population. The second population contained IEs enriched for those that had the ability to bind to CHO-745 WT cells. This allowed the identification of differences between IEs that were able to bind specifically to a receptor of interest and those

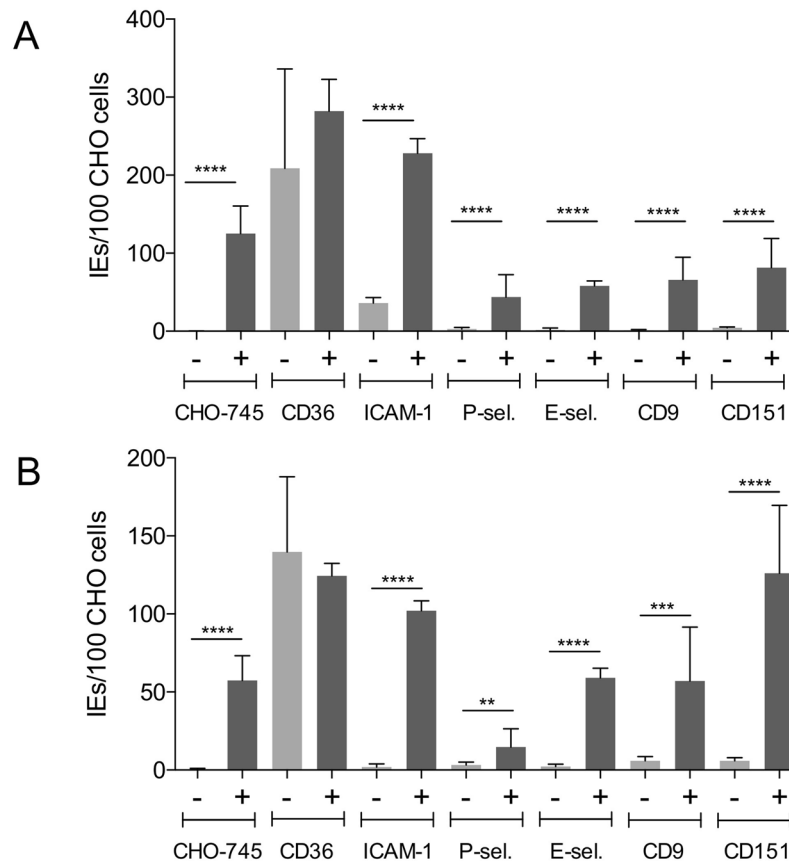


**Figure 1.** The binding capacity of *P. falciparum* isolates IT4 and 3D7 to wild type CHO-745 cells and to various endothelial receptors before (–) and after (+) enrichment for binding to a receptor of interest. CHO-745 cells expressing the receptor of interest on their surface were used to analyse the binding capacity of isolates IT4 (A) and 3D7 (B). After incubation of trophozoite-stage IEs with the respective CHO-745 cell monolayer seeded on a coverslip, the slides were washed, fixed with 1% glutaraldehyde and finally stained with Giemsa stain. Bars represent the mean number  $\pm$  SD of IEs that bound per 100 CHO-745 cells, as determined by light microscopic evaluation. CHO-745, non-transfected CHO-745 WT cells. Statistical significance was determined using the unpaired *t*-test; \*\**p* < 0.01, \*\*\**p* < 0.001, \*\*\*\**p* < 0.0001.

that bound unknown surface proteins/structures on CHO-745 WT cells. The third population comprised IEs that were enriched on the receptors of interest (Supplementary Fig. S4A–S4C). Using NGS (next generation sequencing), the transcriptome profiles of the parasite populations were determined and evaluated using bioinformatics tools, focusing on *var* gene expression in the early ring-stage parasites (Supplementary Fig. S4D).

The analysis of the transcriptome of the IT4 isolate after long-term culturing (IT4\_Ctrl) revealed that nearly all *var* genes were expressed (Fig. 2A and Supplementary Table S1). Most IT4 parasites expressed group A IT4\_var35 and group C IT4\_var34 genes (Fig. 2A and D). These two genes were also highly expressed in all other IT4 populations analysed (Figs 2A/E, 3A/D and 4A/B, S6A) and were therefore excluded from subsequent analyses. The other highly expressed *var* genes in the IT4\_Ctrl population were IT4\_var66 (representing 39% of all *var* transcripts), followed by IT4\_var67 (11%), IT4\_var21 (7%) and IT4\_var65 (5%) (Fig. 2A and B).

After six to seven rounds of enrichment, an IT4 parasite population with a strong binding capacity to CHO-745 WT cells was selected (Supplementary Fig. S3A–S3D). The transcriptome profile of this population showed a significant enrichment of parasite populations that expressed group B IT4\_var14, IT4\_var32A, IT4\_var32B and IT4\_var29 genes, and the group C IT4\_var28 gene (representing 5%, 24%, 30%, 4% and 27%, respectively, of all *var* transcripts in the transcriptome) (Fig. 2A,C–E).

As a proof of concept, the transcriptomes of populations enriched for parasites with the ability to bind to ICAM-1 and CD36 were analysed. In the IT4 population enriched for ICAM-1-binding parasites, significant expression of the group B *var* genes IT4\_var41, IT4\_var16 and IT4\_var63, and group C *var* gene IT4\_var01, was observed (Supplementary Fig. S5A and Table S1). IT4\_var01 was the dominant transcript (representing 90% of all *var* transcripts). In addition, there was a tendency to express group B IT4\_var27 gene (Fig. 2F and G). Except for IT4\_var63, all the detected *var* genes encode a DBL $\beta$ 5 domain known to mediate binding to ICAM-1<sup>36,37</sup> (Fig. 2H).

The IT4 population enriched for CD36-binding parasites displayed a mixed *var* transcript profile in which IT4\_var01, which encodes a protein containing the CD36-binding domain, represented 22% of all *var* transcripts

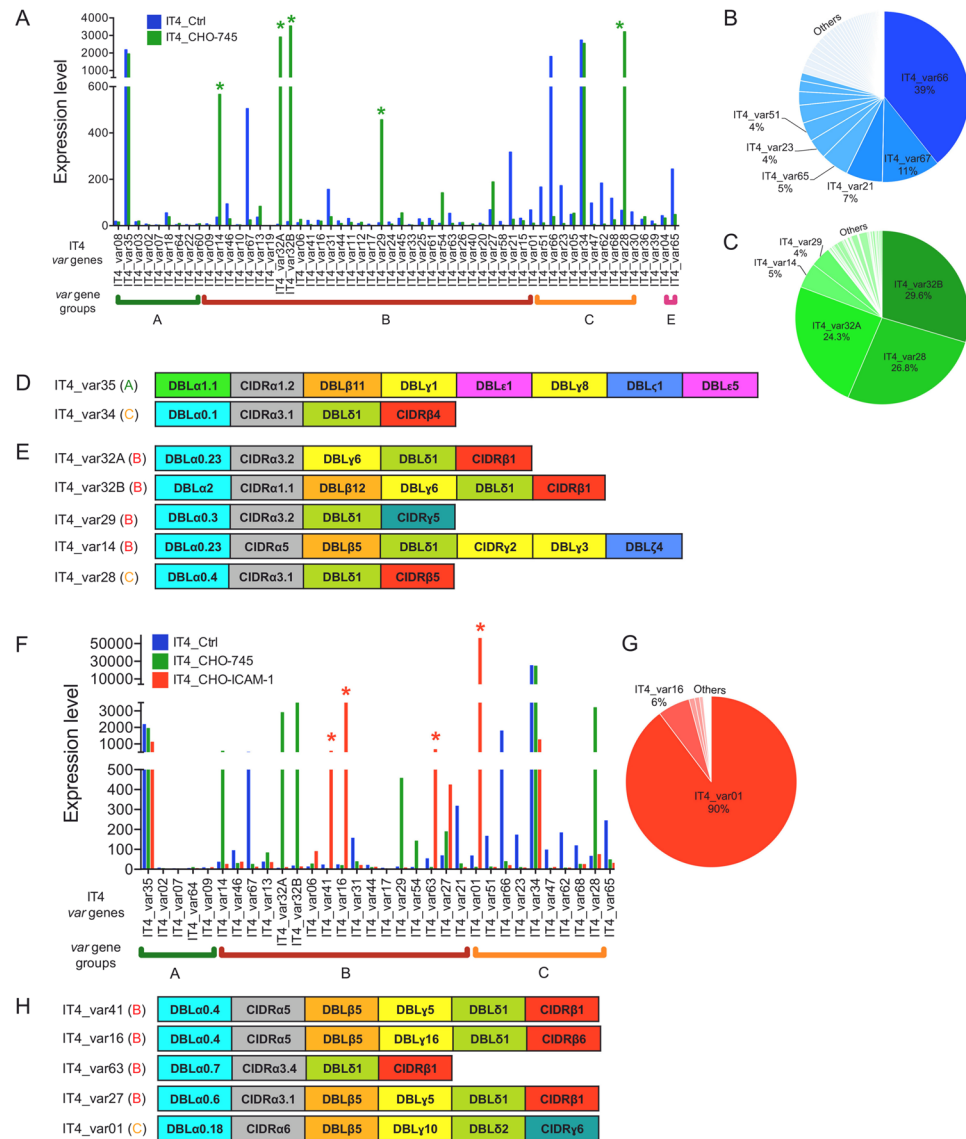


**Figure 2.** Enrichment of a *P. falciparum* IT4 population for parasites binding to CHO-745 WT cells (IT4\_CHO-745) and for ICAM-1-binding parasites (IT4\_CHO-745-ICAM-1). (A) The expression of a selected set of *var* genes in long-term cultured IT4 parasites (IT4\_Ctrl) and IT4\_CHO-745 (expression level is defined as average of the normalized read counts). *var* genes with a significantly higher expression in IT4\_CHO-745 than in IT4\_Ctrl are marked by green stars ( $\text{padj} < 0.05$ ). (B) Distribution of *var* gene expression in the IT4\_Ctrl population. (C) Distribution of *var* gene expression in the IT4\_CHO-745 population. IT4\_var34 and IT4\_var35 were excluded from the analyses. (D) Schematic representation of *PfEMP1* proteins encoded by IT4\_var35 and IT4\_var34 genes with high expression levels in all the investigated parasite populations. (E) Schematic representation of *PfEMP1* proteins encoded by *var* genes whose expression was significantly increased in IT4\_CHO-745 parasites compared with gene expression in long-term cultured IT4 parasites (IT4\_Ctrl) and an IT4 population enriched for parasites binding to CHO-745 cells (IT4\_CHO-745). *var* genes with significantly increased expression in IT4\_CHO-745-ICAM-1 parasites are marked by red stars ( $\text{padj} < 0.05$ ). (F) The expression of a selected set of *var* genes in IT4\_CHO-745-ICAM-1 parasites compared with gene expression in long-term cultured IT4 parasites (IT4\_Ctrl) and an IT4 population enriched for parasites binding to CHO-745 cells (IT4\_CHO-745). *var* genes with significantly increased expression in IT4\_CHO-745-ICAM-1 parasites are marked by red stars ( $\text{padj} < 0.05$ ). (G) Distribution of *var* gene expression in the IT4\_CHO-745-ICAM-1 population. IT4\_var34 and IT4\_var35 were excluded from the analyses. (H) Schematic representation of *PfEMP1* proteins encoded by IT4\_var41, IT4\_var16, IT4\_var63, IT4\_var01 and IT4\_var27 genes whose expression was increased in IT4\_CHO-745-ICAM-1 in comparison with IT4\_Ctrl and IT4\_CHO-745 parasites.

(Supplementary Figs S5B, S6A–C and Table S1). The fact that ca. 80% of all *var* genes encode proteins with the CD36-binding domain<sup>8</sup> hinders the dominance of a specific *var* gene in the transcriptome profile.

Enrichment of the IT4 populations for P-selectin-binding parasites (Supplementary Fig. S5C and Table S1) resulted in populations where the expression of group A IT4\_var02 and IT4\_var07 genes was significantly higher (adjusted  $p$ -value ( $\text{padj}$ )  $< 0.05$ ) than in the other two populations (IT4\_Ctrl and IT4\_CHO-745) (Fig. 3A). IT4\_var02 was the dominant *var* transcript (15% of all *var* transcripts). This was followed by IT4\_var32A, IT4\_var32B

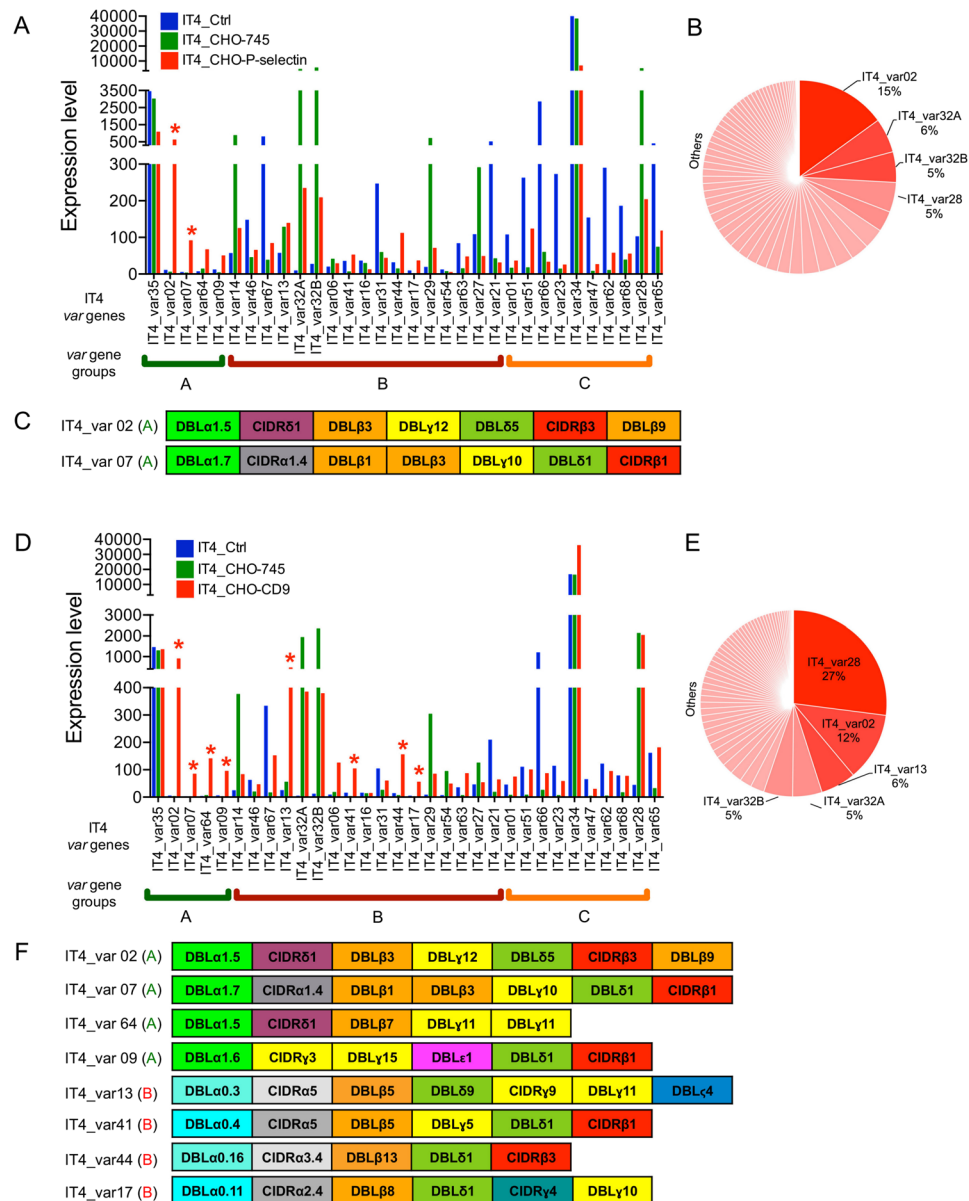


**Figure 3.** Enrichment of a *P. falciparum* IT4 population for P-selectin-binding parasites (IT4\_CHO-745-P-selectin) and for CD9-binding parasites (IT4\_CHO-745-CD9). **(A)** The expression of a selected set of *var* genes in IT4\_CHO-745-P-selectin parasites in comparison with long-term cultured IT4 parasites (IT4\_Ctrl) and an IT4 population enriched for parasites binding to CHO-745 cells (IT4\_CHO-745) (expression level is defined as average of the normalized read counts). *var* genes with significantly increased expression in IT4\_CHO-745-P-selectin parasites are marked by red stars ( $p_{adj} < 0.05$ ). **(B)** Distribution of *var* gene expression in the IT4\_CHO-745-P-selectin population. IT4\_var34 and IT4\_var35 genes were excluded from the analyses. **(C)** Schematic representation of PfEMP1 proteins encoded by IT4\_var02 and IT4\_var07 genes with a significantly higher expression in IT4\_CHO-745-P-selectin than in IT4\_Ctrl and IT4\_CHO-745 parasites. **(D)** The expression of a selected set of *var* genes in IT4\_CHO-745-CD9 parasites in comparison with long-term cultured IT4 parasites (IT4\_Ctrl) and an IT4 population enriched for parasites binding to CHO-745 cells (IT4\_CHO-745). *var* genes with significantly increased expression in IT4\_CHO-745-CD9 parasites are marked by red stars ( $p_{adj} < 0.05$ ). **(E)** Distribution of *var* gene expression in the IT4\_CHO-745-CD9 population. IT4\_var34 and IT4\_var35 were excluded from the analyses. **(F)** Schematic representation of PfEMP1 proteins encoded by IT4\_var02, IT4\_var07, IT4\_var64, IT4\_var09, IT4\_var13, IT4\_var41, IT4\_var44 and IT4\_var17 genes with a significantly higher expression in IT4\_CHO-745-CD9 than in IT4\_Ctrl and IT4\_CHO-745 parasites.



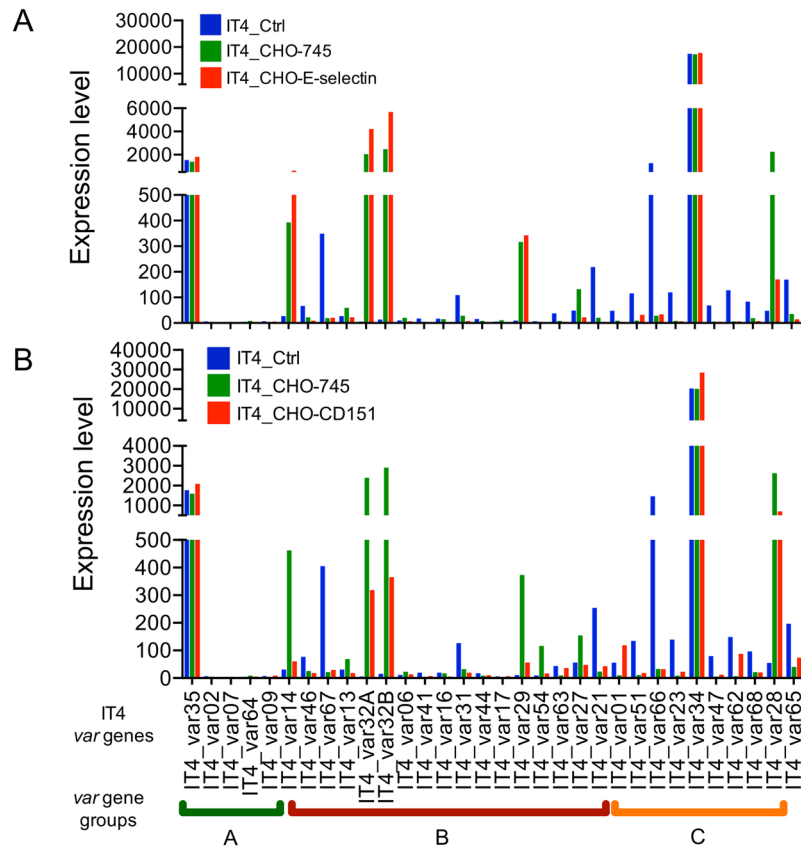


**Figure 4.** Enrichment of a *P. falciparum* IT4 population for E-selectin- and CD151-binding parasites (IT4\_CHO-E-selectin and IT4\_CHO-CD151, respectively). The expression of a selected set of *var* genes in IT4\_CHO-745-E-selectin (A) and IT4\_CHO-745-CD151 parasites (B) compared with long-term cultured IT4 parasites (IT4\_Ctrl) and an IT4 population enriched for parasites binding to CHO-745 cells (IT4\_CHO-745) (expression level is defined as average of the normalized read counts).

and IT4\_var28 transcripts (6%, 5% and 5%, respectively) (Fig. 3B), those were also dominant transcripts within IT4\_CHO-745 population, suggesting that they were not specific to the P-selectin-binding parasites' population. Both IT4\_var02 and IT4\_var07 are group A *var* genes; the head structure of the encoded *PfEMP1* proteins lacks the CD36-binding domain<sup>8</sup>. Instead, the IT4\_var02 *PfEMP1* variant contains two DCs, DC16 (DBL $\alpha$ 1.5-CIDR $\delta$ 1) and DC5 (DBL $\gamma$ 12-DBL $\delta$ 5-CIDR $\beta$ 3-DBL $\beta$ 39), and the IT4\_var07 *PfEMP1* variant contains DC13 (DBL $\alpha$ 1.7-CIDR $\alpha$ 1.4) (Fig. 3C).

Compared with the IT4\_Ctrl and IT4\_CHO-745 populations, eight *var* genes were differentially expressed in the IT4 population enriched for CD9-binding parasites ( $p_{adj} < 0.0001$ ) (Fig. 3D, Supplementary Fig. S5D and Table S1). Four of these (IT4\_var02, IT4\_var07, IT4\_var64 and IT4\_var09) were group A *var* genes, and the other four (IT4\_var13, IT4\_var41, IT4\_var44 and IT4\_var17) were group B *var* genes. The dominant *var* transcript was IT4\_var28 (27%), followed by IT4\_var02 (12%), IT4\_var13 (6%), IT4\_var32A (5%) and IT4\_var32B (5%) (Fig. 3B). Three of the dominant *var* genes (IT4\_var28, IT4\_var32A and IT4\_var32B) were also highly expressed in IT4\_CHO-745 parasites, and were therefore suggested not to be specific for the IT4\_CD9 population. The domain structure of proteins encoded by the four differentially expressed group A *var* genes comprises a head structure with the unique DBL $\alpha$ 1 domains, and CIDR $\delta$ 1 (in IT4\_var02 and IT4\_var64), CIDR $\alpha$ 1.4 (in IT4\_var07) or DBL $\gamma$ 3 (in IT4\_var09). The four group B variants contain the classical head structure responsible for CD36 binding; in addition, IT4\_var13- and IT4\_var41-encoded proteins have an ICAM-1-binding domain (Fig. 3F).

The enrichment for the ability to bind E-selectin and CD151 resulted in an IT4 population that highly expressed IT4\_var14, IT4\_var32A, IT4\_var32B and IT4\_var28 genes. High similarity with the *var* gene expression profile of the IT4\_CHO-745 population was observed (Fig. 4A, B). These results might suggest that both IE populations (IT4\_CHO-E-selectin and IT4\_CHO-CD151) were selected based on binding to an unknown receptor/structure on the CHO-745 WT cell surface, rather than based on their ability to bind E-selectin or CD151, respectively (Supplementary Table S1).

***var* gene expression profiles in enriched 3D7 parasite populations.** The long-term 3D7 isolate culture (3D7\_Ctrl) analysed in this study had a stable *var* gene expression profile, with nearly all *var* genes expressed (Fig. 5A). The PFL0030c *var* gene dominated with 16%, followed by PF08\_0103, PFL1960w and MAL6P1.4 (15%, 8% and 5%, respectively) (Fig. 5B). Transcriptome analyses of the 3D7 population enriched for CHO-745

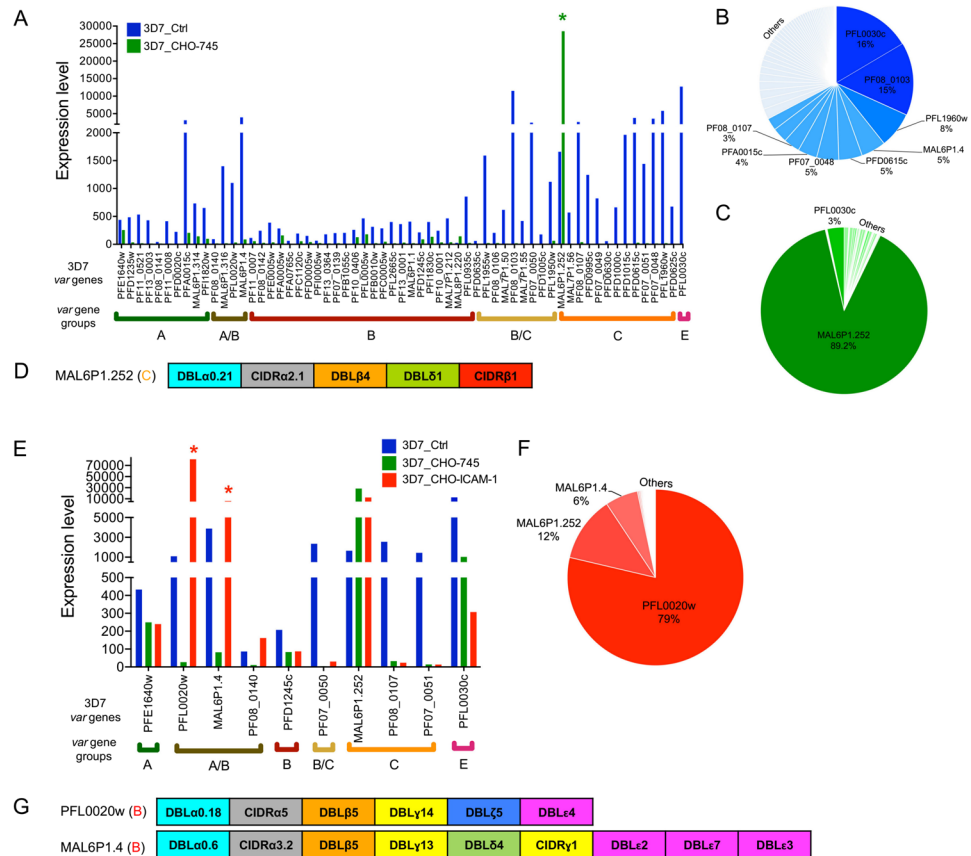


**Figure 5.** Enrichment of a *P. falciparum* 3D7 population for parasites binding to CHO-745 WT cells (3D7\_CHO-745) and for ICAM-1-binding parasites (3D7\_CHO-ICAM-1). (A) *var* gene expression in long-term cultured 3D7 parasites (3D7\_Ctrl) and 3D7\_CHO-745 parasites (expression level is defined as average of the normalized read counts). A *var* gene with significantly increased expression in 3D7\_CHO-745 parasites in comparison with 3D7\_Ctrl parasites is marked by a green star ( $\text{padj} < 0.05$ ). (B) Distribution of *var* gene expression in the 3D7\_Ctrl population. (C) Distribution of *var* gene expression in the 3D7\_CHO-745 population. (D) Schematic representation of *PfEMP1* protein encoded by the MAL6P1.252 gene with significantly increased expression in 3D7\_CHO-745 parasites. (E) The expression of a selected set of *var* genes in 3D7\_CHO-745-ICAM-1 parasites in comparison with long-term cultured 3D7 parasites (3D7\_Ctrl) and a 3D7 population enriched for parasites binding to CHO-745 cells (3D7\_CHO-745). *var* genes with significantly increased expression in the 3D7\_CHO-745-ICAM-1 parasites are marked by red stars ( $\text{padj} < 0.05$ ). (F) Distribution of *var* gene expression in the 3D7\_CHO-745-ICAM-1 population. (G) Schematic representation of *PfEMP1* proteins encoded by PFL0020w and MAL6P1.4 genes with significantly higher expression in 3D7\_CHO-745-ICAM-1 than in 3D7\_Ctrl and 3D7\_CHO parasites.

cell-binding parasites (3D7\_CHO-745) revealed differential expression of MAL6P1.252 ( $\text{padj} \leq 0.05$ ) in comparison with the 3D7\_Ctrl population (Supplementary Table S2). MAL6P1.252 was the dominant *var* transcript (89% of all *var* transcripts), followed by PFL0030c (only 3%) (Fig. 5A and C). The predicted protein encoded by MAL6P1.252 contains the classical head structure required for binding to CD36 (Fig. 5D).

Parasite populations enriched for ICAM-1-binding parasites differentially expressed the group B *var* genes PFL0020w (79% of all *var* transcripts) and MAL6P1.4 (6% of all *var* transcripts) in comparison with the two control populations (Fig. 5E and F; Supplementary Table S2). These two *var* genes encode *PfEMP1* molecules that contain DBLβ5 domains known to bind to ICAM-1 (Fig. 5G). High expression was also noted for MAL6P1.252. Although MAL6P1.252 contains a CD36-binding domain, an ICAM-1-binding domain is not present (Fig. 5D).

Results of the enrichment of a 3D7 population for CD36-binding parasites were the same as for the IT4 isolate, i.e., no differentially expressed genes were detected in comparisons with the 3D7\_Ctrl and 3D7\_CHO-745 populations (Supplementary Fig. S7A and Table S2). The 3D7\_CD36 population predominantly expressed PF07\_0050 (39% of all *var* transcripts), followed by MAL6P1.252 (15%), PF08\_0107 (16%) and PF07\_0051 (10%) (Supplementary Fig. S7B). These four *var* genes encode *PfEMP1* variants that contain CIDRα2–6 domains responsible for CD36 binding (Supplementary Fig. S7C).

Figure 6A–D demonstrates our attempts at enriching the 3D7 population for parasites binding to P-selectin, E-selectin, CD9 and CD151. The expression of all *var* genes was dramatically reduced except for the MAL6P1.252 gene, which was highly expressed in all enriched populations. In all of the enriched populations the expression profiles were comparable with those in the 3D7\_CHO-745 population (Supplementary Tables S11–S14).

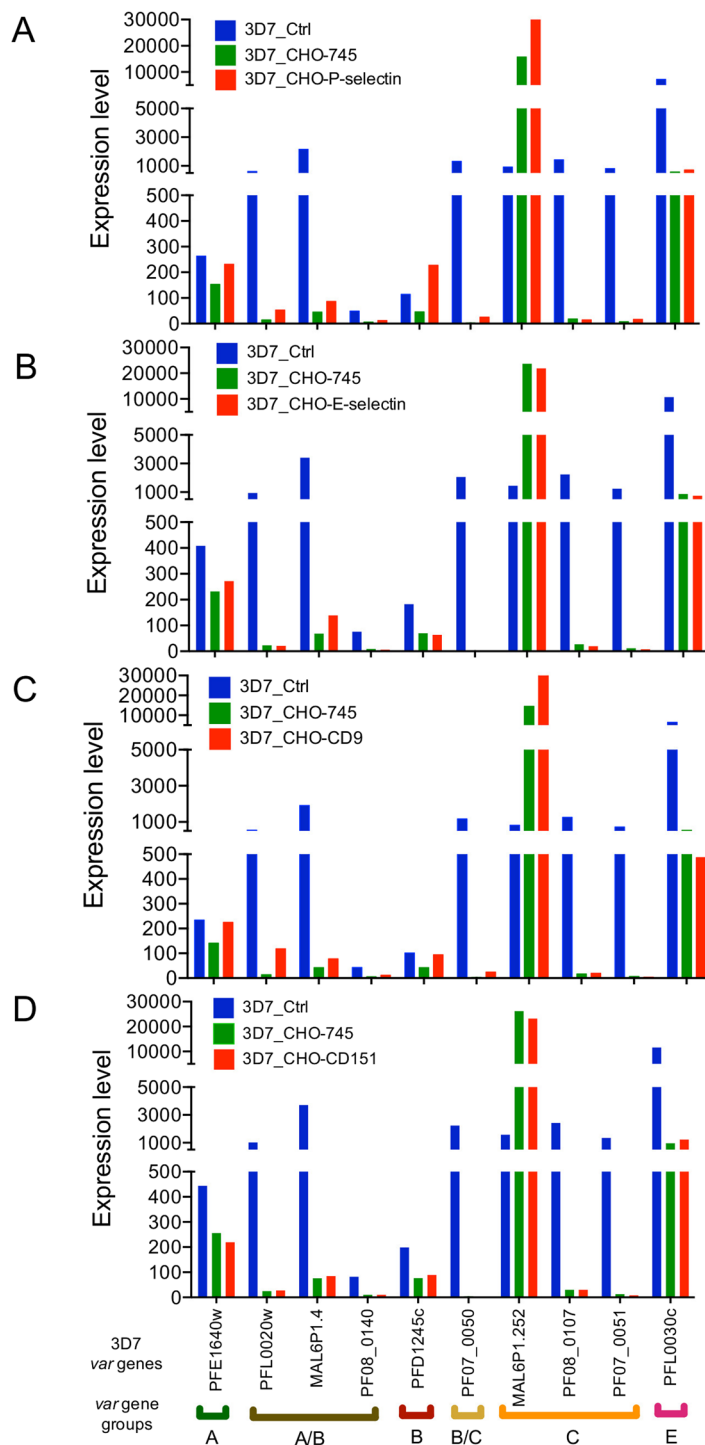


**Figure 6.** Enrichment of a *P. falciparum* 3D7 population for selectin- and tetraspanin-binding parasites. The expression of a selected set of *var* genes in parasite populations enriched for parasites binding to P-selectin (A), E-selectin (B), CD9 (C) or CD151 (D), in comparison with long-term cultured 3D7 parasites (3D7\_Ctrl) and a 3D7 population enriched for parasites binding to CHO-745 cells (3D7\_CHO-745) (expression level is defined as average of the normalized read counts).

**Non-*var* multi-copy gene family profiles in enriched parasite populations.** Although the current study was designed with a focus on the expression of the *var* genes during the early ring-stage (6–8 h after invasion), it also allowed comparative expression analysis of other multi-copy gene families at this time point. The majority of genes belonging to the *rif*, *stevor*, *pfmc2tm* or *surf* families were either not expressed or expressed at very low levels in the various parasite populations at the investigated time point.



Considering IT4 isolate (Supplementary Tables S3–S9, S17), three *rif* genes, PFIT\_0400300.1, PFIT\_0400300.2 and PFIT\_bin04400, were approximately equal and relatively high expressed in all parasite populations. Expression of two *rif* genes, PFIT\_0616600 and PFIT\_bin00500, tended to be higher in the IT4\_CHO-ICAM-1 population. In the population enriched for CD36-binding parasites, significant high expression of one *rif* gene (PFIT\_0811700) was observed. In addition, the PFIT\_0537100, PFIT\_1150800 and PFIT\_bin04900 *rif* genes tended to be highly expressed. In the transcriptome of IT4\_CHO-P-selectin IEs, significant expression of the PFIT\_0801600 *rif* gene was observed. PFIT\_bin07800 *rif*, PFIT\_bin05800 *stevor* and PFIT\_1301050 *surf* tended to be highly expressed. The expression of three *surf* genes, PFIT\_0803400, PFIT\_1301000 and PFIT\_0422600, was significantly higher in the IT4\_CHO-P-selectin population. In the IT4\_CD9 population, four *rif* genes (PFIT\_0801600, PFIT\_0800200, PFIT\_bin03400 and PFIT\_bin07800) and four *surf* genes (PFIT\_0803400, PFIT\_1301000, PFIT\_0422600 and PFIT\_1301050) were differentially expressed. In addition, the expression of two *stevor* genes, PFIT\_0901600 and PFIT\_bin05800, was also higher in the IT4\_CHO-CD9 population than that in the respective controls (Supplementary Table S17).

Within 3D7 isolate (Supplementary Tables S10–S16, S18), the expression levels of two *rif* genes, PF3D7\_0401600.1 and PF3D7\_0401600.2, were approximately equal and high in all the parasite populations. Interestingly, most *rif* genes were highly expressed in 3D7\_CHO-745 populations. Considering the *stevor* genes, PF3D7\_0102100 tended to be highly expressed in the CD9-binding enriched population and PF3D7\_0115400 was highly expressed in the ICAM-1-binding enriched population. The expression of only one *surf* gene (PF3D7\_1301800) was equally high in all the enriched parasite populations and in the controls. *Pfmc2tm* gene family was expressed at various levels in the control and enriched populations (Supplementary Table S18).

## Discussion

A complete *PfEMP1* interactome map is still not available. In the current study, we were aiming to predict putative *P. falciparum* *var* genes that encode ligands for different endothelial receptors. We established and combined three approaches (cellular, molecular and bioinformatics) that enabled us to perform a comprehensive analysis of different parasite populations enriched for parasites binding to different endothelial receptors exposed on the surface of transgenic CHO-745 cells. The robustness of the methods used in this study was confirmed by analysing the transcriptomes of two different isolate populations (IT4 and 3D7) enriched for ICAM-1- and CD36-binding parasites. The respective parasite populations expressed *var* genes that encode *PfEMP1* molecules containing binding domains for ICAM-1 and CD36, respectively (DBL35 and CIDR $\alpha$ 2–6, respectively). As was also shown by Petter and colleagues, the dominant transcript in parasites selected on ICAM-1 was PFL0020w<sup>49</sup>. In the case of the IT4 isolate, as previously described, all six *PfEMP1* molecules (IT4\_var01, IT4\_var13, IT4\_var14, IT4\_var16, IT4\_var27 and IT4\_var41) containing the DBL35 domain could bind to ICAM-1<sup>36, 37, 50</sup>. Of these, IT4\_var01, IT4\_var16, IT4\_var27 and IT4\_var41 were identified as dominant transcripts in ICAM-1-enriched parasites in this study, with 90% of all *var* transcripts attributed to IT4\_var01.

In addition to the interaction of IEs with the CD36 and ICAM-1 receptors, it was also reported that IEs can adhere to other molecules, including lectins, P-selectin and E-selectin, and tetraspanins, CD9 and CD151<sup>25, 39, 43, 44</sup>. However, in contrast to ICAM-1 and CD36, *P. falciparum* ligands participating in these binding events are as yet unknown.

In the present study, following comparison with the respective controls, IT4\_var02 was identified as the dominant transcript in IT4 parasite populations enriched for P-selectin- and CD9-binding parasites. The *PfEMP1* variant encoded by this gene contains a head structure with a non-binding CD36 domain forming DC16, followed by DC5. Parasites expressing IT4\_var02 exhibit binding affinity for transformed human bone marrow endothelial cells, and this binding ability could not be inhibited by anti-EPCR antibodies<sup>26</sup>. Furthermore, strong binding affinities of DC5 of the 3D7 isolate (PF11\_0008 gene) and IT4 isolate (IT4\_var02 gene) for transformed bone marrow endothelial cells expressing both ICAM-1 and PECAM-1 were also reported. Inhibition of the binding by anti-ICAM-1 antibodies was not successful; the binding was inhibited by anti-PECAM-1 antibodies<sup>29</sup>.

Moreover, IT4\_var07 was differentially expressed in both IT4\_CHO-P-selectin and IT4\_CHO-CD9 populations. The IT4\_var07-encoded *PfEMP1* variant contains DC13<sup>8</sup>. High levels of DC13 transcript were reported in patients with severe malaria<sup>33</sup>. IEs expressing DC13 bind to different endothelial cell types, and it has been proposed that DC13 mediates binding to EPCR via the CIDR $\alpha$ 1 domain subclass<sup>24, 26</sup>. Binding of parasite populations expressing IT4\_var07 to endothelial cell lines in the brain, lung and dermis under shear stress conditions was also demonstrated. Surprisingly, when EPCR was blocked, the binding to bone marrow and lung endothelial cells was inhibited, but the IEs continued to bind to the brain and dermal endothelial cells, confirming the versatility of IE receptor affinities<sup>51</sup>.

In this study, we observed eight highly expressed *var* genes within CD9 enriched populations, which is somehow puzzling. Four of the genes encode for group A *PfEMP1* (IT4\_var02, IT4\_var64, IT4\_var09 and IT4\_var07) and the rest encode for group B *PfEMP1* (IT4\_var44, IT4\_var13, IT4\_var17 and IT4\_var41), rendering some difficulty to predict the exact interacting *PfEMP1* domain(s).

The question of whether P-selectin and CD9 play a role in cerebral malaria (CM) requires further investigation. In *Plasmodium berghei*-infected mice, which can be used as a model of experimental CM, mice lacking P-selectin are protected from malaria-induced death<sup>52, 53</sup>. Up-regulation of P-selectin in the endothelial lining of several organs was reported for a murine *P. berghei* infection. However, the importance of P-selectin in CM is controversial; one study showed up-regulation of P-selectin in the brain vessels of malaria-susceptible mice but not in CM-resistant mice, whereas another study reported a significant increase in P-selectin levels in resistant mice in comparison with control mice<sup>52, 53</sup>. Elevated levels of soluble P-selectin in the sera of patients with severe malaria in comparison with patients with non-severe symptoms were also reported<sup>54</sup>.

Recently, CD9 was identified as a new interaction partner of IEs<sup>25</sup>; however, it is not known whether CD9 plays a role in the development of malarial pathogenesis. CD9 plays a role in the leukocyte aggregation cascade, where it mediates leukocyte aggregation in the brain through endothelial adhesive platforms (EAPs), i.e., adhesive clusters containing CD9 and ICAM-1. Upon leukocyte binding via CD9, the EAPs rise above the endothelial surface to facilitate leukocyte capture<sup>55</sup>. CD9 also plays a role in some infectious diseases, like in HIV or bacterial infections<sup>56,57</sup>. All these data indicate the prime importance of the identification of the parasite's ligand(s) in the interactions mentioned above.

We were unable to identify a parasite population binding to E-selectin. Until now, neither the role of E-selectin in CM nor its *PfEMP1* ligand has been identified. Post-mortem brain examination of patients who died from CM in Thailand revealed up-regulation of E-selectin in the endothelial lining. In the same study, it was also possible to select IEs for binding to E-selectin<sup>40</sup>. In a study from the same region, 60 patient *Plasmodium* isolates from patients were tested for adherence to CD36, ICAM-1, VCAM-1 and E-selectin; the binding to the latter two was negligible<sup>46</sup>. Furthermore, no binding of E-selectin was detected under flow conditions<sup>41</sup>. Recently, Janes and colleagues tested the binding capacity of IEs that expressed group A *var* genes for CHO-745 transfectants with superficial E-selectin expression; only minimal binding was observed<sup>39</sup>. The controversial data mentioned above may support the observations in the current study that suggest that E-selectin plays only a minor or no role in the cytoadhesion of IEs to the vascular endothelium.

Similarly to CD9, CD151 was recently shown to bind IEs<sup>25</sup>. Based on the current analysis of the two laboratory isolates, we conclude that CD151 has only minor relevance for cytoadhesion to IEs because the dominant *var* gene transcripts in populations enriched for CD151-binding parasites were exactly the same as those in the CHO-745 WT-grown populations.

A high and almost identical expression pattern of two *var* genes, IT4\_var35 (*var1*, pseudogene) and IT4\_var34, was observed in all IT4 populations investigated. IT4\_var35 is a truncated gene that lacks the exon 2 sequence and has a shortened acidic terminal segment<sup>8</sup>. It has been postulated that pseudogenes act as a *var* diversity archive, similarly to variant surface glycoproteins in *Trypanosoma*<sup>58</sup>. We also observed a high and unchanging expression of PFIT\_bin09700. BLAST analysis identified this mRNA as a fragment of IT4\_var34; it appears that this gene is fragmented (exists as two fragments) in the IT4 isolate used in this study, which might affect its translation to a full-length surface *PfEMP1* protein.

We observed an interesting binding phenotype of IEs to wild-type CHO-745 cells. Especially at the first rounds of enrichment large numbers of IEs adhered in a clump-like fashion to morphologically abnormal (rarely occurring) CHO-745 cells. These cells were larger than normal<sup>59</sup> with many cytoplasmic vacuoles, large or multiple nuclei, an increased number of lysosomes and an extended Golgi network. The cells with such abnormal morphology are known as 'senescent cells'; they lose their ability to multiply but remain metabolically active<sup>48,60,61</sup>. Strong adhesive molecules are present on the surface of senescent endothelial cells<sup>62</sup>. For example, the expression of a gene encoding CD44 is higher in senescent cells than in younger cells. A higher binding capacity of monocytes clusters to CD44 for senescent endothelial cells was also reported<sup>63</sup>.

In another study, the binding of IEs to wild-type CHO-745 cells was also observed. The authors attributed this to the presence of NCAM on the surface of CHO-745 cells because the binding was partially blocked by NCAM-specific antibodies. Interestingly, they also observed clumpy collections of IEs and described them as 'macro aggregates' composed of hundreds of IEs<sup>64</sup>. The answer to the question of whether CD44, NCAM, both or additional proteins are responsible for the interaction with IEs remains elusive<sup>65</sup>.

The expression of MAL6P1.252 in the four different 3D7 populations (3D7\_CHO-P-selectin-/E-selectin-/CD9-/CD151) was surprising. Frank and colleagues concluded that the *var* genes possess different intrinsic switching rates depending on the *var* gene subtype. They used a clonal parasite population that exclusively expressed the central *var* gene MAL6P1.252. No change in *var* gene expression was observed in this clone over 13 weeks of continuous growth, indicating an immeasurably low off-rate for this locus<sup>66</sup>. Thus, presumably, the populations expressing MAL6P1.252 interact with a receptor on CHO-745 cells. Because of the continuous selection and the low expression of group A *var* genes in the starting culture, these populations dominated and, given their low switching *var* rate, it was impossible to select any other parasite population that could bind P-selectin or CD9.

Recent studies suggest that *PfEMP1* is not the main variable surface antigen during a chronic *P. falciparum* infection<sup>67</sup>. The analysis of the expression profiles of other multi-copy gene families revealed an interesting differential expression of *surf* genes in populations enriched for the P-selectin- and CD9-binding parasites. SURFIN was recently described as a polymorphic antigen encoded by 10 *surf* genes, and it was suggested that SURFINS are crucial for parasite survival, but this is still under investigation<sup>12</sup>. The *rif* genes are transcribed 12–27 h post invasion<sup>68</sup>, but, even though the parasite populations were harvested at earlier time points in the current study, we observed a tendency for high expression of some of the *rif* genes in CD36-, ICAM-1-, P-selectin- and CD9-binding populations. This emphasises the many open questions regarding the exact functions of RIFIN proteins in cytoadhesion.

Taken together, the current study predicted *PfEMP1* candidates that might interact with P-selectin and CD9. The most interesting finding herein was that the identified *PfEMP1* variants belong to group A *PfEMP1*s, which is a frequent finding in *Plasmodium* isolates from patients with severe malaria. As a proof of concept, ICAM-1 and CD36 ligands were identified. Moreover, we were not able to identify binding partners for E-selectin and CD151. The reason for this may be that the binding to these receptors is weaker, than the binding to the unknown receptor on CHO-745 cells or they do not play a role in cytoadhesion of IEs. Finally, an interesting phenotype concerning the binding of IEs to senescent cells in the CHO-745 cell culture was observed. Further investigations are required to uncover the molecular backgrounds of these interactions, especially the respective *PfEMP1* domains responsible for binding.

## Methods

**Parasite culture.** *P. falciparum* isolates IT4 (FCR3S1.2) and 3D7 were cultivated with human O+ erythrocytes (5% haematocrit) in the presence of 10% human serum A+ (Interstate blood bank, Hamburg, Germany), according to standard procedures<sup>69</sup>. Parasite cultures were synchronised once a week using 5% sorbitol<sup>70</sup>.

**CHO-745 cell transfection and culture.** CHO-745 cells defective in glycosaminoglycan biosynthesis (CHO-745; American Type Culture Collection no. CRL-2242) were used in this study. CD36, ICAM-1, P-selectin and E-selectin cDNAs were cloned into pAcGFP1-N1 (Clontech Laboratories), whereas CD9 and CD151 were cloned into pEGFP-N1 (Clontech Laboratories). CHO-745 cells were transfected using Lipofectamine 2000 (Invitrogen) according to the manufacturer's protocol. The plasmids were kindly provided by Rolf Horstmann (Bernhard Nocht Institute for Tropical Medicine, Hamburg), and the transfectants were generated as previously described<sup>25,71</sup>.

Transfected CHO-745 cells were cultivated at 37 °C and under 5% CO<sub>2</sub> in Ham's F-12 medium (PAA) supplemented with 10% foetal calf serum (PAA) and penicillin-streptomycin. Neomycin (G418; stock concentration 50 mg/mL; with final concentration, 0.7 mg/mL) was used as a selective agent for the transfected cells.

**Immunofluorescence analyses of endothelial receptors.** CHO-745 cells expressing the receptors under investigation were grown on coverslips and fixed with 2% followed by 4% para-formaldehyde. Each CHO-745 cell line was labelled using the respective antibody ( $\alpha$ CD62E (1:33, R&D Systems),  $\alpha$ CD62P (1:33, Santa Cruz Biotechnology),  $\alpha$ CD151 (1:33, Rolf Horstmann, BNITM, Hamburg, Germany),  $\alpha$ CD54 (1:50, eBioscience),  $\alpha$ CD9 (1:50, Chemicon International),  $\alpha$ CD36 (1:50, R&D Systems), which was then conjugated to Alexa-Fluor-594 (Invitrogen) as a secondary antibody. Nuclei were stained with Hoechst-33342 staining (1:1000) (Sigma). The cover slips were then mounted with DAKO fluorescent mounting medium and examined under a fluorescent microscope (Zeiss Axioskop2 plus-Carl Zeiss AG and EVOS FL-Thermofisher). Cells incubated with secondary antibody alone did not show fluorescence in any experiment (Supplementary Fig. S2).

**Static binding assay.** The static cytoadhesion assays were performed as previously described<sup>25</sup>. The transfected CHO-745 cells were seeded onto coverslips (13 mm) at a density of 30,000 cells/mL 2 d before the assay. On the day of the assay the phenotype and confluence level of CHO-745 cells was controlled under light microscope. The assay was performed with 50–100% (ideal: 90%) confluent monolayer CHO-745 cells. Highly synchronised trophozoite-stage parasite culture (5% parasitaemia, 1% haematocrit) was suspended in the binding medium (RPMI 1640 medium supplemented with 2% glucose, pH 7.2). The parasite cell suspension was added to CHO-745 cells expressing only GFP (to allow IE pre-absorption) for 1 h at 37 °C and under 5% CO<sub>2</sub>, with orbital shaking every 15 min. Next, the pre-absorbed suspension was incubated with receptor-expressing CHO-745 cells for 1 h at 37 °C and under 5% CO<sub>2</sub>, with gentle shaking in all directions every 15 min. The coverslips were then washed with the binding medium to remove unbound erythrocytes. Cells adhering to the coverslips were fixed with 1% glutaraldehyde in phosphate-buffered saline for 30 min at room temperature. Finally, the cells were stained with a filtered Giemsa/Weisser buffer solution (1:10). The number of adherent IEs was determined by counting 300 CHO-745 cells under a light microscope. Assays were conducted three times in triplicate. The data are expressed as the mean with standard deviation (SD).

**Selection and enrichment for IEs binding to the receptors of interest.** Two days before the assay, the desired transfected-CHO-745 cell line as well as the non-transfected CHO-745 cells (for preabsorption) were cultivated in culture flasks. On the day of the assay highly synchronised trophozoite-stage IEs (10% parasitaemia), were suspended in binding medium (5% haematocrit). Confluence level was controlled under light microscope (50–100% confluent monolayer). The parasite cell suspension was added to non-transfected CHO-745 cells (to allow IE pre-absorption) for 1 h at 37 °C (5% CO<sub>2</sub>), with orbital shaking every 15 min. Next, the pre-absorbed suspension was incubated with receptor-expressing CHO-745 cells for 1 h at 37 °C (5% CO<sub>2</sub>), with gentle shaking in all directions every 15 min. Thereafter, unbound IEs were removed by 5–8 washes of the binding medium. The binding of IEs to the CHO-745 cells was confirmed by examination under an inverted microscope. To enable further growth of the selected parasite populations, bound IEs were co-incubated with CHO-745 cells and cultivated following standard *Plasmodium* procedures for 24 h. On the following day, ring-stage IEs were harvested; this was followed by a depletion of the remaining CHO-745 cells using the BIOCOLL separating solution (Biochrom™). The selected IEs were cultured until 10% parasitaemia, and the entire procedure was repeated.

**RNA purification, library preparation and transcriptome analysis.** Ring-stage IEs were harvested, rapidly lysed in a 20-times higher volume of pre-warmed (37 °C) TRIzol® (Invitrogen) and stored at –80 °C. RNA was isolated using the PureLink™ RNA Mini Kit (ThermoFisher Scientific), according to the manufacturer's instructions. The quality and quantity of total RNA were assessed using the Agilent™ 2100 Bioanalyzer System with Agilent™ RNA 6000 Pico kit (Agilent Technologies). To avoid contamination with genomic DNA, the samples were treated with TURBO™ DNase (ThermoFisher Scientific) followed by magnetic bead enzymatic wash using Agencourt RNA Clean XP (Beckman Coulter). To ensure deep sequencing of mRNA, rRNA was depleted using the Ribo-Zero™ Kit (Illumina), according to the manufacturer's instructions. The rRNA-depleted RNA samples were then purified using the RNeasy™ MinElute Cleanup Kit (Qiagen). The concentration of RNA as well as the quality of mRNA in the treated samples were assessed using the Agilent 2100™ Bioanalyzer System (Agilent™ RNA 6000 Pico kit for mRNA assay; Agilent Technologies).

The IT4 isolate libraries were constructed using the ScriptSeq™ v2 RNA-Seq Library Preparation Kit (Illumina) according to the manufacturer's protocols. The abundance and size distribution of the fragments within the libraries were checked using the Agilent™ 2100 Bioanalyzer System (Agilent™ High Sensitivity DNA Kit; Agilent Technologies). The indexed libraries were multiplexed into one pool (4 nM concentration) of four

different libraries. The pooled library was denatured and diluted according to the protocol described in the Illumina user guide. Next-generation sequencing runs were performed using Illumina Miseq with paired-end sequences. FastQC (Babraham Bioinformatics) was used for quality control, and the reads with  $\geq 30$  Phred quality score were included in the analysis.

For the 3D7 isolate, RNA was sent to BGI Genomics Co (Shenzhen, China). There, the Illumina Hiseq 4000 platform was used for sequencing, with the libraries multiplexed in two different lanes. Transcriptomes of *P. falciparum* strains IT4 and 3D7 were downloaded from PlasmoDB (<http://plasmodb.org/plasmo/>), and clean reads were aligned to these transcripts using Bowtie<sup>72</sup>. DESeq 1.18 was used for read normalisation<sup>73</sup>. Read pairs coherently aligned to one transcript were counted using samtools<sup>74</sup>. The *var* gene repertoire of *P. falciparum* strains IT4 and 3D7 is listed in Supplementary Tables S19 and S20.

**Statistical analysis.** Statistical significance of the results of the binding assays was established using an unpaired *t*-test. Differential gene expression analysis was performed using a generalised linear model in DESeq 1.18<sup>75</sup>. Differentially expressed genes were defined as those that are significantly expressed in the receptor-enriched parasite population compared to the two controls (IT4/3D7\_Ctrl, IT4/3D7\_CHO-745). Benjamini-Hochberg (BH) method (basic R package version 3.3.2) was used to declare statistical significance of the analysis done for multicopy gene families<sup>76</sup>. This generated a BH adjusted *p*-value (padj). For this adjustment. The largest *p*-value ( $p < (i/m)Q$ ) was considered significant and consequently all *p*-values smaller than it were also considered significant, even the ones that were bigger than their BH adjusted *p*-value<sup>76</sup>.

In the pie charts, the average expression of each *var* gene was displayed as a proportion of the combined *var* gene expression in each population, calculated using MS Excel 2016. Since the *var* genes IT4\_var34 and IT4\_var35 are most probably co-expressed in all IT4 parasite populations analysed, their expression level was deduced from the combined *var* gene expression to assess the relative expression of other *var* genes in each population.

## References

1. WHO. World malaria report 2016. (2016).
2. Miller, L. H., Baruch, D. I., Marsh, K. & Doumbo, O. K. The pathogenic basis of malaria. *Nature* **415**, 673–679 (2002).
3. Rowe, J. A., Claessens, A., Corrigan, R. A. & Arman, M. Adhesion of *Plasmodium falciparum*-infected erythrocytes to human cells: molecular mechanisms and therapeutic implications. *Expert Rev Mol Med* **11**, e16 (2009).
4. Yipp, B. G. *et al.* Src-family kinase signaling modulates the adhesion of *Plasmodium falciparum* on human microvascular endothelium under flow. *Blood* **101**, 2850–2857 (2003).
5. Jambou, R. *et al.* *Plasmodium falciparum* adhesion on human brain microvascular endothelial cells involves transmigration-like cup formation and induces opening of intercellular junctions. *PLoS Pathog* **6**, e1001021 (2010).
6. Jenkins, N. *et al.* *Plasmodium falciparum* intercellular adhesion molecule-1-based cytoadherence-related signaling in human endothelial cells. *J Infect Dis* **196**, 321–327 (2007).
7. Hvid, L. & Jensen, A. T. PfEMP1 - A Parasite Protein Family of Key Importance in *Plasmodium falciparum* Malaria Immunity and Pathogenesis. *Adv Parasitol* **88**, 51–84, doi:10.1016/bs.apar.2015.02.004 (2015).
8. Rask, T. S., Hansen, D. A., Theander, T. G., Gorm Pedersen, A. & Lavstsen, T. *Plasmodium falciparum* erythrocyte membrane protein 1 diversity in seven genomes—divide and conquer. *PLoS computational biology* **6**, doi:10.1371/journal.pcbi.1000933 (2010).
9. Lavazec, C., Sanyal, S. & Templeton, T. J. Expression switching in the stevor and Pfmc-2TM superfamilies in *Plasmodium falciparum*. *Mol Microbiol* **64**, 1621–1634 (2007).
10. Sam-Yellowe, T. Y. *et al.* A *Plasmodium* gene family encoding Maurer's cleft membrane proteins: structural properties and expression profiling. *Genome Res* **14**, 1052–1059 (2004).
11. Cheng, Q. *et al.* stevor and rif are *Plasmodium falciparum* multicopy gene families which potentially encode variant antigens. *Mol Biochem Parasitol* **97**, 161–176 (1998).
12. Winter, G. *et al.* SURFIN is a polymorphic antigen expressed on *Plasmodium falciparum* merozoites and infected erythrocytes. *J Exp Med* **201**, 1853–1863 (2005).
13. Leech, J. H., Barnwell, J. W., Miller, L. H. & Howard, R. J. Identification of a strain-specific malarial antigen exposed on the surface of *Plasmodium falciparum*-infected erythrocytes. *J Exp Med* **159**, 1567–1575 (1984).
14. Pasternak, N. D. & Dzikowski, R. PfEMP1: an antigen that plays a key role in the pathogenicity and immune evasion of the malaria parasite *Plasmodium falciparum*. *Int J Biochem & Cell Biol* **41**, 1463–1466 (2009).
15. Baruch, D. I. *et al.* Cloning the *P. falciparum* gene encoding PfEMP1, a malarial variant antigen and adherence receptor on the surface of parasitized human erythrocytes. *Cell* **82**, 77–87 (1995).
16. Su, X. Z. *et al.* The large diverse gene family var encodes proteins involved in cytoadherence and antigenic variation of *Plasmodium falciparum*-infected erythrocytes. *Cell* **82**, 89–100 (1995).
17. Voss, T. S. *et al.* A var gene promoter controls allelic exclusion of virulence genes in *Plasmodium falciparum* malaria. *Nature* **439**, 1004–1008 (2006).
18. Gardner, M. J. *et al.* Sequence of *Plasmodium falciparum* chromosomes 2, 10, 11 and 14. *Nature* **419**, 531–534, doi:10.1038/nature01094 (2002).
19. Smith, J. D., Subramanian, G., Gamain, B., Baruch, D. I. & Miller, L. H. Classification of adhesive domains in the *Plasmodium falciparum* erythrocyte membrane protein 1 family. *Mol Biochem Parasitol* **110**, 293–310 (2000).
20. Smith, J. D. *et al.* Identification of a *Plasmodium falciparum* intercellular adhesion molecule-1 binding domain: a parasite adhesion trait implicated in cerebral malaria. *Proc Natl Acad Sci USA* **97**, 1766–1771 (2000).
21. Kraemer, S. M. & Smith, J. D. Evidence for the importance of genetic structuring to the structural and functional specialization of the *Plasmodium falciparum* var gene family. *Mol Microbiol* **50**, 1527–1538 (2003).
22. Kraemer, S. M. *et al.* Patterns of gene recombination shape var gene repertoires in *Plasmodium falciparum*: comparisons of geographically diverse isolates. *BMC Genomics* **8**, 45 (2007).
23. Lavstsen, T., Salanti, A., Jensen, A. T., Arnot, D. E. & Theander, T. G. Sub-grouping of *Plasmodium falciparum* 3D7 var genes based on sequence analysis of coding and non-coding regions. *Malar J* **2**, 27 (2003).
24. Avril, M., Brazier, A. J., Melcher, M., Sampath, S. & Smith, J. D. DC8 and DC13 var genes associated with severe malaria bind avidly to diverse endothelial cells. *PLoS Pathog* **9**, e1003430, doi:10.1371/journal.ppat.1003430 (2013).
25. Esser, C. *et al.* Evidence of promiscuous endothelial binding by *Plasmodium falciparum*-infected erythrocytes. *Cell Microbiol* **16**, 701–708, doi:10.1111/cmi.12270 (2014).
26. Turner, L. *et al.* Severe malaria is associated with parasite binding to endothelial protein C receptor. *Nature* **498**, 502–505, doi:10.1038/nature12216 (2013).
27. Serghides, L., Smith, T. G., Patel, S. N. & Kain, K. C. CD36 and malaria: friends or foes? *Trends Parasitol* **19**, 461–469 (2003).



28. Chakravorty, S. J. & Craig, A. The role of ICAM-1 in *Plasmodium falciparum* cytoadherence. *Eur J Cell Biol* **84**, 15–27, doi:10.1016/j.ejcb.2004.09.002 (2005).
29. Berger, S. S. *et al.* *Plasmodium falciparum* expressing domain cassette 5 type PfEMP1 (DC5-PfEMP1) bind PECAM1. *PLoS ONE* **8**, e69117, doi:10.1371/journal.pone.0069117 (2013).
30. Beeson, J. G. *et al.* Antibodies to variant surface antigens of *Plasmodium falciparum*-infected erythrocytes and adhesion inhibitory antibodies are associated with placental malaria and have overlapping and distinct targets. *J Infect Dis* **189**, 540–551, doi:10.1086/381186 (2004).
31. Robinson, B. A., Welch, T. L. & Smith, J. D. Widespread functional specialization of *Plasmodium falciparum* erythrocyte membrane protein 1 family members to bind CD36 analysed across a parasite genome. *Mol Microbiol* **47**, 1265–1278 (2003).
32. Lau, C. K. *et al.* Structural conservation despite huge sequence diversity allows EPCR binding by the PfEMP1 family implicated in severe childhood malaria. *Cell host & microbe* **17**, 118–129, doi:10.1016/j.chom.2014.11.007 (2015).
33. Lavstsen, T. *et al.* *Plasmodium falciparum* erythrocyte membrane protein 1 domain cassettes 8 and 13 are associated with severe malaria in children. *Proc Natl Acad Sci USA* **109**, E1791–1800, doi:10.1073/pnas.1120455109 (2012).
34. Jespersen, J. S. *et al.* *Plasmodium falciparum* var genes expressed in children with severe malaria encode CIDRalpha1 domains. *EMBO Mol Med* **8**, 839–850, doi:10.15252/emmm.201606188 (2016).
35. Mkumbaye, S. I. *et al.* The severity of *Plasmodium falciparum* infection is associated with transcript levels of var genes encoding EPCR-binding PfEMP1. *Infect Immun.* doi:10.1128/IAI.00841-16 (2017).
36. Bengtsson, A. *et al.* A novel domain cassette identifies *Plasmodium falciparum* PfEMP1 proteins binding ICAM-1 and is a target of cross-reactive, adhesion-inhibitory antibodies. *J Immunol* **190**, 240–249, doi:10.4049/jimmunol.1202578 (2013).
37. Howell, D. P. *et al.* Mapping a common interaction site used by *Plasmodium falciparum* Duffy binding-like domains to bind diverse host receptors. *Mol Microbiol* **67**, 78–87 (2008).
38. Oleinikov, A. V. *et al.* High throughput functional assays of the variant antigen PfEMP1 reveal a single domain in the 3D7 *Plasmodium falciparum* genome that binds ICAM1 with high affinity and is targeted by naturally acquired neutralizing antibodies. *PLoS Pathog* **5**, e1000386 (2009).
39. Janes, J. H. *et al.* Investigating the host binding signature on the *Plasmodium falciparum* PfEMP1 protein family. *PLoS Pathog* **7**, e1002032, doi:10.1371/journal.ppat.1002032 (2011).
40. Ockenhouse, C. F. *et al.* Human vascular endothelial cell adhesion receptors for *Plasmodium falciparum*-infected erythrocytes: roles for endothelial leukocyte adhesion molecule 1 and vascular cell adhesion molecule 1. *J Exp Med* **176**, 1183–1189 (1992).
41. Udomsangpetch, R. *et al.* Promiscuity of clinical *Plasmodium falciparum* isolates for multiple adhesion molecules under flow conditions. *J Immunol* **158**, 4358–4364 (1997).
42. Ho, M. *et al.* Characterization of *Plasmodium falciparum*-infected erythrocyte and P-selectin interaction under flow conditions. *Blood* **91**, 4803–4809 (1998).
43. Yipp, B. G. *et al.* Differential roles of CD36, ICAM-1, and P-selectin in *Plasmodium falciparum* cytoadherence *in vivo*. *Microcirculation* **14**, 593–602 (2007).
44. Senczuk, A. M., Reeder, J. C., Kosmala, M. M. & Ho, M. *Plasmodium falciparum* erythrocyte membrane protein 1 functions as a ligand for P-selectin. *Blood* **98**, 3132–3135 (2001).
45. Ockenhouse, C. F., Magowan, C. & Chulay, J. D. Activation of monocytes and platelets by monoclonal antibodies or malaria-infected erythrocytes binding to the CD36 surface receptor *in vitro*. *J Clin Invest* **84**, 468–475 (1989).
46. Udomsangpetch, R. *et al.* Receptor specificity of clinical *Plasmodium falciparum* isolates: nonadherence to cell-bound E-selectin and vascular cell adhesion molecule-1. *Blood* **88**, 2754–2760 (1996).
47. Peacocke, M. & Campisi, J. Cellular senescence: a reflection of normal growth control, differentiation, or aging? *J Cell Biochem* **45**, 147–155, doi:10.1002/jcb.240450205 (1991).
48. Campisi, J. & d'Adda di Fagagna, F. Cellular senescence: when bad things happen to good cells. *Nat Rev Mol Cell Biol* **8**, 729–740, doi:10.1038/nrm2233 (2007).
49. Petter, M. *et al.* Expression of *P. falciparum* var genes involves exchange of the histone variant H2A.Z at the promoter. *PLoS Pathog* **7**, e1001292, doi:10.1371/journal.ppat.1001292 (2011).
50. Springer, A. L., Smith, L. M., Mackay, D. Q., Nelson, S. O. & Smith, J. D. Functional interdependence of the DBLbeta domain and c2 region for binding of the *Plasmodium falciparum* variant antigen to ICAM-1. *Mol Biochem Parasitol* **137**, 55–64 (2004).
51. Gillrie, M. R. *et al.* Diverse functional outcomes of *Plasmodium falciparum* ligation of EPCR: potential implications for malarial pathogenesis. *Cell Microbiol* **17**, 1883–1899, doi:10.1111/cmi.12479 (2015).
52. Chang, W. L. *et al.* P-selectin contributes to severe experimental malaria but is not required for leukocyte adhesion to brain microvasculature. *Infect Immun* **71**, 1911–1918, doi:10.1128/iai.71.4.1911-1918.2003 (2003).
53. Combes, V. *et al.* Pathogenic role of P-selectin in experimental cerebral malaria - Importance of the endothelial compartment. *Am J Pathol* **164**, 781–786, doi:10.1016/S0002-9440(10)63166-5 (2004).
54. Facer, C. A. & Theodoridou, A. Elevated Plasma-Levels of P-Selectin (Gmp-140 Cd62p) in Patients with Plasmodium-Falciparum Malaria. *Microbiol Immunol* **38**, 727–731 (1994).
55. Franz, J. *et al.* Nanoscale Imaging Reveals a Tetraspanin-CD9 Coordinated Elevation of Endothelial ICAM-1 Clusters. *PLoS ONE* **11**, doi:ARTN e014659810.1371/journal.pone.0146598 (2016).
56. Gordon-Alonso, M. *et al.* Tetraspanins CD9 and CD81 modulate HIV-1-induced membrane fusion. *J Immunol* **177**, 5129–5137 (2006).
57. van Spriel, A. B. & Figdor, C. G. The role of tetraspanins in the pathogenesis of infectious diseases. *Microbes Infect* **12**, 106–112, doi:10.1016/j.micinf.2009.11.001 (2010).
58. Marcello, L. & Barry, J. D. Analysis of the VSG gene silent archive in *Trypanosoma brucei* reveals that mosaic gene expression is prominent in antigenic variation and is favored by archive substructure. *Genome Res* **17**, 1344–1352, doi:10.1101/gr.6421207 (2007).
59. Porter, K., Prescott, D. & Frye, J. Changes in surface morphology of Chinese hamster ovary cells during the cell cycle. *J Cell Biol* **57**, 815–836 (1973).
60. Hayflick, L. & Moorhead, P. S. The serial cultivation of human diploid cell strains. *Exp Cell Res* **25**, 585–621 (1961).
61. Robbins, E., Levine, E. M. & Eagle, H. Morphologic changes accompanying senescence of cultured human diploid cells. *J Exp Med* **131**, 1211–1222 (1970).
62. Mun, G. I. & Boo, Y. C. Identification of CD44 as a senescence-induced cell adhesion gene responsible for the enhanced monocyte recruitment to senescent endothelial cells. *Am J Physiol Heart Circ Physiol* **298**, H2102–2111, doi:10.1152/ajpheart.00835.2009 (2010).
63. Lowe, D. & Raj, K. Premature aging induced by radiation exhibits pro-atherosclerotic effects mediated by epigenetic activation of CD44 expression. *Aging Cell* **13**, 900–910, doi:10.1111/accel.12253 (2014).
64. Pouvelle, B. *et al.* Neural cell adhesion molecule, a new cytoadhesion receptor for *Plasmodium falciparum*-infected erythrocytes capable of aggregation. *Infect Immun* **75**, 3516–3522, doi:10.1128/IAI.01852-06 (2007).
65. Andrews, K. T., Adams, Y., Viebig, N. K., Lanzer, M. & Schwartz-Albiez, R. Adherence of *Plasmodium falciparum* infected erythrocytes to CHO-745 cells and inhibition of binding by protein A in the presence of human serum. *Int J Parasitol* **35**, 1127–1134, doi:10.1016/j.ijpara.2005.05.007 (2005).
66. Frank, M., Dzikowski, R., Amulic, B. & Deitsch, K. Variable switching rates of malaria virulence genes are associated with chromosomal position. *Mol Microbiol* **64**, 1486–1498 (2007).



67. Bruske, E. I. *et al.* In Vitro Variant Surface Antigen Expression in *Plasmodium falciparum* Parasites from a Semi-Immune Individual Is Not Correlated with Var Gene Transcription. *PLoS ONE* **11**, e0166135, doi:10.1371/journal.pone.0166135 (2016).
68. Bachmann, A. *et al.* Temporal expression and localization patterns of variant surface antigens in clinical *Plasmodium falciparum* isolates during erythrocyte schizogony. *PLoS ONE* **7**, e49540, doi:10.1371/journal.pone.0049540 (2012).
69. Trager, W. & Jensen, J. B. Human malaria parasites in continuous culture. *Science* **193**, 673–675 (1976).
70. Lambros, C. & Vanderberg, J. P. Synchronization of *Plasmodium falciparum* erythrocytic stages in culture. *J Parasitol* **65**, 418–420 (1979).
71. Bachmann, A. *et al.* Absence of erythrocyte sequestration and lack of multicopy gene family expression in *Plasmodium falciparum* from a splenectomized malaria patient. *PLoS ONE* **4**, e7459 (2009).
72. Langmead, B. & Salzberg, S. L. Fast gapped-read alignment with Bowtie 2. *Nat Methods* **9**, 357–359, doi:10.1038/nmeth.1923 (2012).
73. Ashburner, M. *et al.* Gene ontology: tool for the unification of biology. The Gene Ontology Consortium. *Nat Genet* **25**, 25–29, doi:10.1038/75556 (2000).
74. Li, H. *et al.* The Sequence Alignment/Map format and SAMtools. *Bioinformatics (Oxford, England)* **25**, 2078–2079, doi:10.1093/bioinformatics/btp352 (2009).
75. Anders, S. & Huber, W. Differential expression analysis for sequence count data. *Genome Biol* **11**, R106, doi:10.1186/gb-2010-11-10-r106 (2010).
76. Benjamini, Y., Drai, D., Elmer, G., Kafkafi, N. & Golani, I. Controlling the false discovery rate in behavior genetics research. *Behav Brain Res* **125**, 279–284 (2001).

## Acknowledgements

We thank Susann Ofori, Jürgen Sievertsen, Christa Ehmen and Birgit Förster for technical assistance and Tobias Spielmann for helpful discussion. The work was supported by the Deutscher Akademischer Austauschdienst (DAAD), Leibniz Center Infection, Jürgen Manchot Stiftung and the Deutsche Forschungsgemeinschaft (DFG, Br1744/12-1). The publication of this article was funded by the Open Access Fund of the Leibniz Association.

## Author Contributions

Concept development: N.G.M., A.K.T., E.T., I.B. Experimental work: N.G.M., A.K.T., P.L., L.K.R., M.D., S.W., H.T., T.G. Contributed materials: S.W., A.B., H.T., T.G. Data analysis: N.G.M., S.L., A.K.T., K.S., I.B. Wrote the paper: N.G.M., T.R., T.B., A.B., I.B. All authors reviewed the manuscript.

## Additional Information

**Supplementary information** accompanies this paper at doi:10.1038/s41598-017-04241-3

**Competing Interests:** The authors declare that they have no competing interests.

**Publisher's note:** Springer Nature remains neutral with regard to jurisdictional claims in published maps and institutional affiliations.



**Open Access** This article is licensed under a Creative Commons Attribution 4.0 International License, which permits use, sharing, adaptation, distribution and reproduction in any medium or format, as long as you give appropriate credit to the original author(s) and the source, provide a link to the Creative Commons license, and indicate if changes were made. The images or other third party material in this article are included in the article's Creative Commons license, unless indicated otherwise in a credit line to the material. If material is not included in the article's Creative Commons license and your intended use is not permitted by statutory regulation or exceeds the permitted use, you will need to obtain permission directly from the copyright holder. To view a copy of this license, visit <http://creativecommons.org/licenses/by/4.0/>.

© The Author(s) 2017